Australian Journal of Basic and Applied Sciences, 4(2): 302-313, 2010
ISSN 1991-8178

Metallogeny of Manganese and Ferromanganese Ores in Baft Ophiolitic Mélange, Kerman, Iran

[1]Kouros Heshmatbehzadi, [2]Jamshid shahabpour

[1]Department of Geology, Faculty of Sciences, Shahid Bahonar University of Kerman, P.O. Box 76169133, Kerman, Islamic Republic of Iran
[2]Department of Geology, Shahid Bahonar University of Kerman, P.O. Box 955, Post Cod 76135, Kerman, I.R. Iran.

Abstract: In Kerman region manganese and ferromanganese ores have been reported from Baft ophiolitic mélange.The Baft ophiolitic mélange is part of a series of Cretaceous ophiolitic mélange in the southern edge of the central Iranian microplate. In the Baft area manganese and ferromanganese ores occur at two ore localities, namely, Gugher Mn ore locality in the northwest of Baft, and Gushk Mn ore locality in the south of Baft. The Mn and Fe-Mn ores of the Baft area contain variable amounts of pyrolosite, hematite, goethite, pyrochroite, Fe-Mn silicate and some chalcocite and pyrite. Gangue minerals are cryptocrystalline quartz, amorphous silica, iron rich clay and calcite. The chemical composition of the manganese and ferromanganese ores in the Baft area suggests that the Mn-Fe ores originated mostly from hydrothermal exhalite while passing through the oceanic rocks ores and debouch into the cretaceous Nain-Baft Oceanic crust. These deposits were later obducted and tectonized as part of the Baft ophiolitic mélange.

Key words: Ophiolite; Manganese ore; Baft; Metallogeny; Exhalite.

INTRODUCTION

It is now generally understood that manganese deposits have diverse origins.They can be formed by sedimentary, hydrothermal, hydrogenous and supergene processes. Sedimentary and hydrothermal processes of manganese deposition are well understood. Hydrothermal manganese deposits are, small, while sedimentary manganase deposits may attain a much larger size (Roy, 1992) . Hydrothermal manganese ores may be stratabound or occur as irregular bodies and epithermal veins. They are formed in the marine environment, next to the spreading centers, intraplate seamounts or in subduction-related island arc settings and have been recognized from both modern and ancient geological environments (Roy, 1997).

Manganese and ferromanganese ore deposits are recognized with different age and geological settings in Iran (Shahabpour, 2002).

For example, the Infracambrian Narigan Mn ore deposit in Yazd provience (central Iran) has a volcano exhalative genesis; The Cretaceous Benvid ophiolitic Mn deposit 35 Km south of Nain-Isfahan, with possible sedex genesis and Kamar Talar ophiolitic Mn deposit in Sistan suture zone, east Iran (Arvin and Robinson, 1994). Abundance of ophiolites and their associated Fe-Mn deposits in Iran demands a special attention as far as this ore deposits are concered. However these is a lack data on this matter.

The aim of the present work is to study the genesis of Mn and Fe-Mn ore deposits in Baft Region.

General Geology:

The Baft ophiolitic melange is part of the Tethyan ophiolites which is located in south east of Iran, at the southern extremity of Nain-Baft fault (Fig.1). The Nain–Baft ophiolite complex (Davoudzadeh, 1972; Arvin and Robinson, 1994) is borderd to the northeast by the Urumieh –Dokhtar magmatic assemblage, and to the southwest by Sanandaj –Sirjan metamorphic zone (SSZ).

The Baft ophiolitic mélange has a classic ophiolite pseudo stratigraphy which from bottom to top consists of:

(1) ulteramafic – mafic complex, (2) sedimentary units, (3) metamorphic units.

Corresponding Author: Kouros Heshmatbehzadi, Department of Geology, Faculty of Sciences, Shahid Bahonar University of Kerman, P.O. Box 76169133, Kerman, Islamic Republic of Iran
Tel, Fax:+98(341)3222035, G-mail: k.heshmatbehzadi.pnu@gmail.com

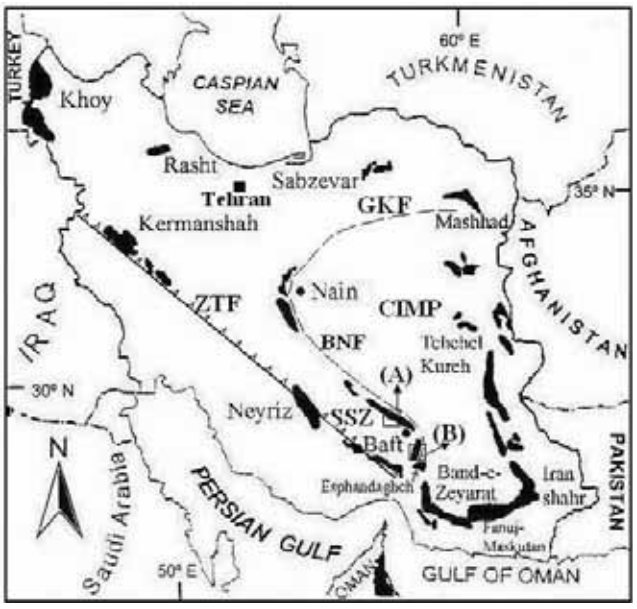

Fig. 1: Map showing locations of major Iranian ophiolites and location of the study areas in Baft ophiolitic mélange (Modified after Hassanipak Hassanipak and Ghazi, 2000).
(A): Gougher Mn ore locality (Fig 2). (B): Goushk Mn ore locality (Fig 3).
BNF: Nain-Baft Fault. CIMP: Centeral Iranian microplate.
GKF: Great Kavir Fault SSZ: Sanandaj- Sirjan zone.
ZTF: Zagros thrust fault.

The ulteramafic- mafic complex consists of serpentinized harzburgite, gabbro, massive diabase, diabase dyke, spilitized pillowlava and basic flowbreccia with angular to subrounded fragments of spilites. The mélange groundmass mainly consist of serpentinized harzburgites, with relicts of orthopyroxenes, dispersed grains of chromite and asbestosis veins in Baft area. In addition there are several chromitite ore bodies with lenticular and podiform structure. Serpentinites are invaded by small gabbro stocks, sometimes only a few meters in diameter. Large gabbro masses are of noritic type, with augite, hypersthene, and plagioclases of labradurite-bytownite composition. These rocks are highly alterd saussuritized and uralitized diabasic rocks mostly crop out in the shape of massive diabase on the serpentinized harzburgite and diabase dyke swarms with NW- SE trend which invade the spilite units. Spilites form blocks and pillow lavas in the ultramafic groundmass. They consists of albitized plagioclases, some clinopyroxene and secondry products.

The sedimentery units contains cretaceous limestone, sandstone and conglomerates. Limestones are represented mostly by biomicrites with a rich pelagic microfauna (Globotruncana gansseri, Globotruncana stuarti, ...) of Campanian-Maesterrichtian age.

The oldest outcropping unit of the Eocene sequence, consisting of sandstones and some conglomerate, is exposed south east of Gugher village (Fig. 2).

The sediments have a turbiditic aspect in places and has sedimentary boundaries with ophiolithic basement rocks. Cretaceous pelagic limestone and Eocene sandstone with a primitive sedimentary boundaries overlies spilitic units.

The metamorphic unit of Paleozoic age, essentially occurs in the 15 km southwest of Gugher village and some occurs also in the south of Gushk Mn ore locality (marble, slate and greenschist). Metamorphic units from bottom to top consists of calcschist, chlorite-sericite schist (amphibole schist), biotite schist, marble and crystalline limestone in Gugher area.

This units are metamorphic slabs from SSZ, that tectonically overturned on ophiolitic mélange. In some places for example along of shear zone and shear fault zone, metamorphism (about greenschist facies) occurs on ophiolitic units, in which is younger than ophiolitic units.

From tectonical setting Baft ophiolitic mélange is a back arc basine (Shahabpour, 2005) that with tectonical force, from southwest and accords with zagros folding are setting along of Nain-Baft fault at late cretaceous to late Eocene.

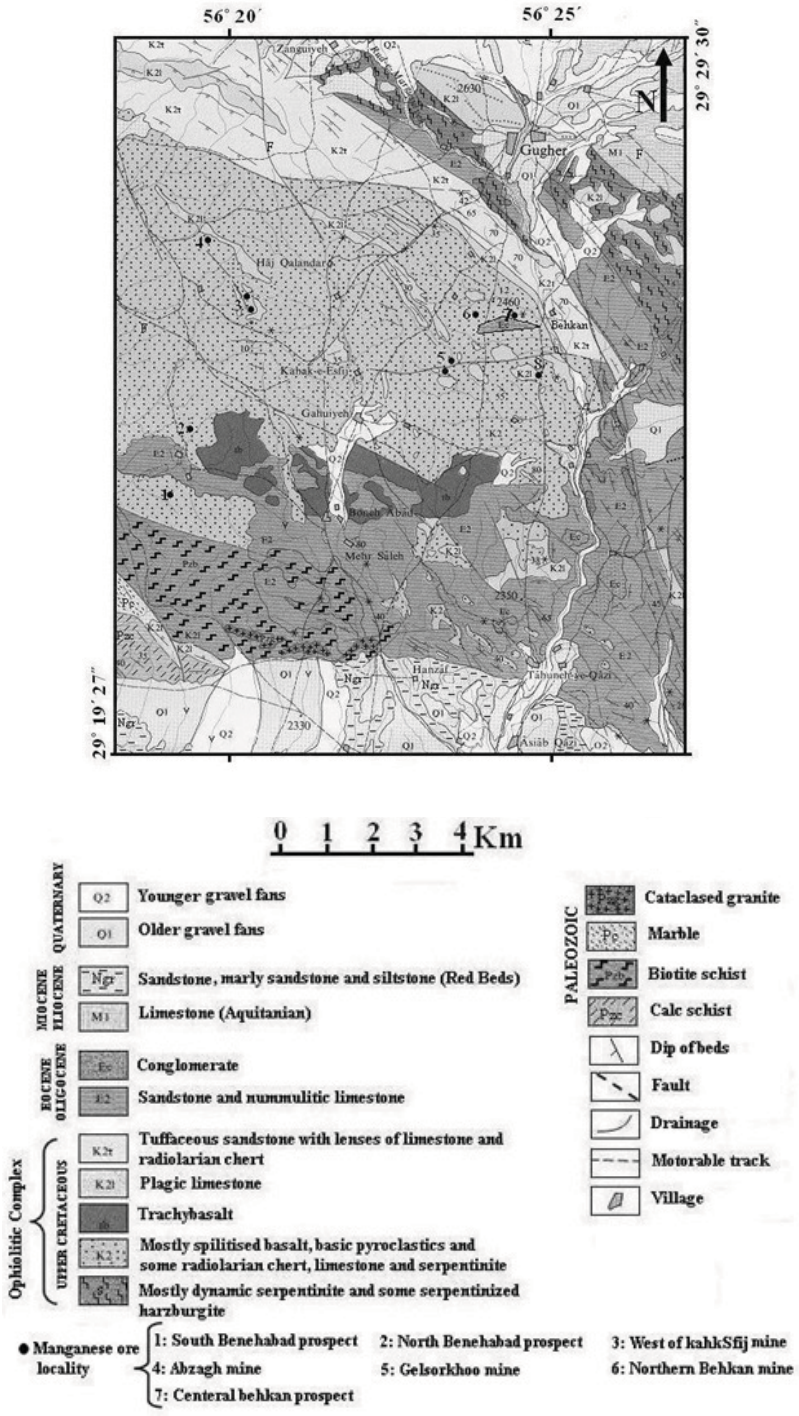

Fig. 2: Geological and Mn metallogenic map of Gugher ore locality (modified after Mijalkovic and Cvetic, 1972.

Morphology and Texture:

In the Baft area manganese and ferromanganese ores occur at two ore localites, namely, Gugher ore locality (Abzagh, Kahkesfij, Behkan, Benehabad and Gelsorkhoo) in the northwest of Baft (Fig. 2) and Gushk

Mn ore locality (Benehhavuieh, southern Gushk and Zaghdar) in the south of Baft (Fig. 3).

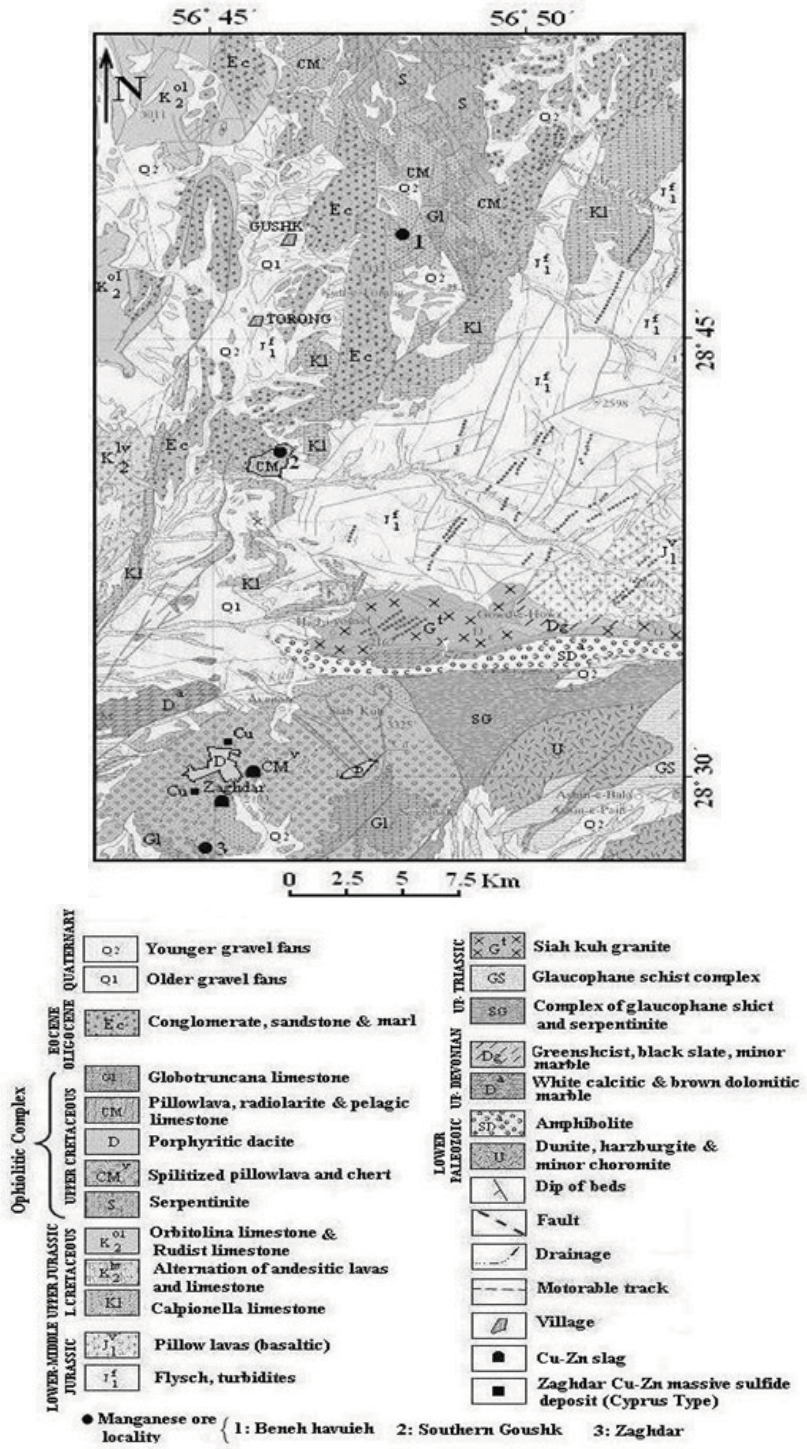

Fig. 3: Geological and Mn metallogenic map of Gushk ore locality (modified after Houshmandzadeh *et al.*, 1994.

Manganese ore bodies usually are hosted by basalt and iron chert or massive limestone. The manganese and ferromanganese ores of these ore localities contain variable amounts of pyrolusite, hematite, goethite, pyrochroite, tephroite (Mn_2SiO_4), Fe-Mn silicate and some high chalcocite, pyrite, chalcopyrite, tennorite and smithsonite. Gangue minerals are cryptocrystalline quartz, amorphous silica, iron rich clay, alunite and calcite.

Field studies, on Mn deposites in Baft ophiolitic mélange show that these deposits commonly have lenticular, layered and sometimes cross cutting veins morphology (Fig. 4). Field studies and geochemical data show that lenticular and vein ores in Gugher and Gushk Mn ore bodies originated mainly from a hydrothermal exhalite source, and were formed in the vicinity of the sea floor spreading centers, within the Nain–Baft oceanic crust. Layered Mn ores this deposited as proximal and distal orebodies.

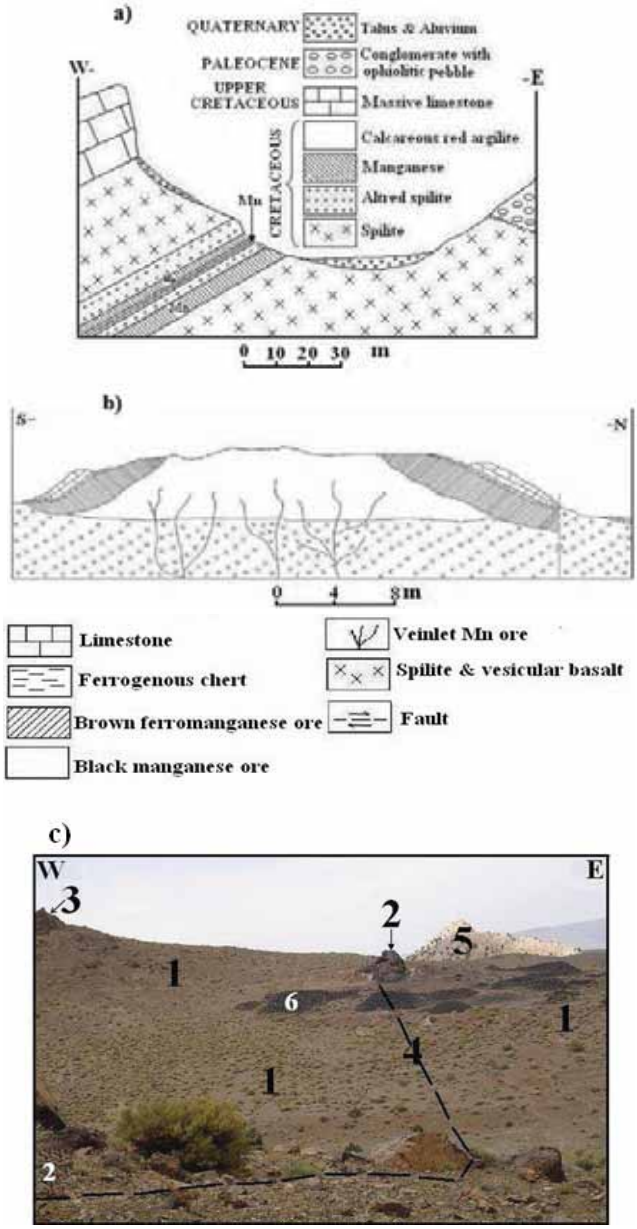

Fig. 4: Different structure at Baft manganese ore deposits. a) Layerd manganese ore (interlayerd with basalt) at southern Behkan Mn prospect. b) Lenticular shape Mn ore deposit at Gelsorkhu mine. c) Vein type Mn ore at northern Behkan mine, (1- Spilite, 2- Manganese Vein, 3- Diabase dyke swarm, 4- Strike of Mn vein, 5- Cretaceous limestone, 6- extracted Manganese ore).

The textures such as breccia, cockade, veined and crustification (Table. 1) are found in the Baft manganese and ferromanganese ores (Fig. 5). These ore textures, the lenticular shapes and geochemical data (section) in Baft manganese ore suggest a submariane exhalite origin for the deposit.

Table 1: Morphological and characteristics of the Baft manganese ore bodies.

Mn localities	Host rocks	Morphology	Texture
Northern Behkan	Spilite & Iron chert	Cross-cutting veins	Breccia, Cockade, Veinlet
Southern Behkan	Vesicular basalt	Intera layerd	Cockade, Colloform
Northern Gelsorkhoo	Spilite & Limestone	Layerd	Colloform
Southern Gelsorkhoo	Spilite & Limestone	Lenticular shape	Breccia, Cockade, Crustification Colloform, Cockade,
West of Kahk sfij	Spilite & Limestone	Lenticular & Layerd	Crustification Breccia,Crustification
Beneh abad	Spilite & Limestone	Lenticular	Colloform Breccia, Colloform,
Beneh havouieh	Spilite & Iron chert	Lenticular	Cockade
Southern Goushk	Spilite & Iron chert	Layerd	Colloform, Cockade
Zaghdar	Spilite, Chert & Limestone	Layerd	Colloform, Cockade

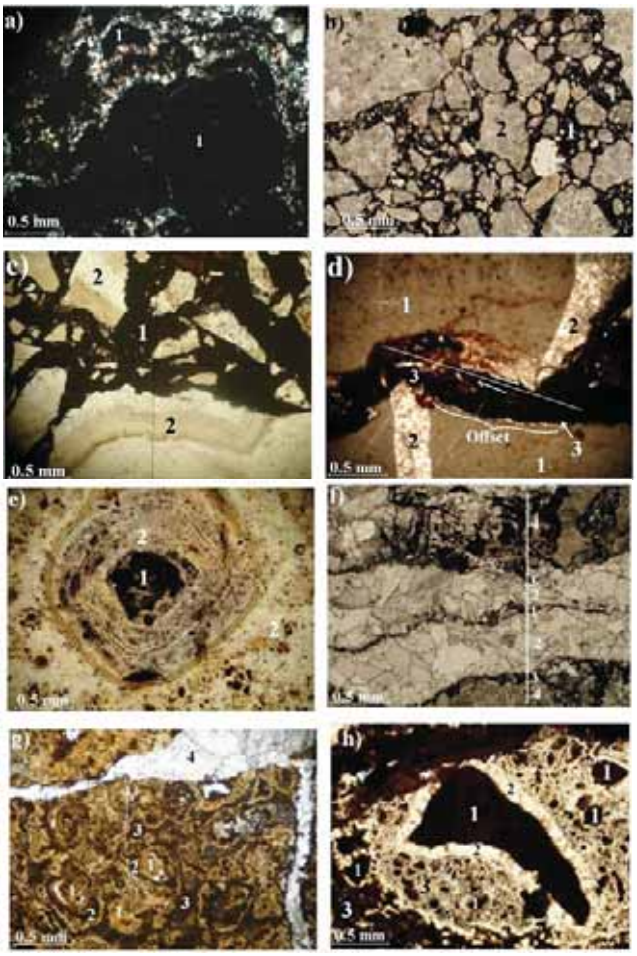

Fig. 5: Texture of the Baft manganese and ferromanganese ores.
a) Colloform texture:1- Pyrolusite nucleous, 2- microcrystalline quartz. b) Breccia texture: 1- Fe-Mn oxides(matrix), 2- microcrystaline quartz. c) Breccia texture: 1- Fe-Mn oxides(matrix), 2- Angular particles of microcrystaline quartz & amorphous silica with primary colloform texture. d) Vein texture (fracture filling): 1- amorphous silica, 2- calcite vein, 3- Fe-Mn oxides vein. e) Colloform texture in manganese nodules: 1- Fe-Mn oxides (nucleous), 2- microcrystaline quartz laminations and relictes of Mn oxide with colloform texture. f) Crustification texture: 1- Fe-Mn oxides, 2- calcite, 3- Fe-Mn oxides, 4- microcrystaline quartz and Fe-Mn oxides. g) Cockade texture: 1- amorphous silica (nucleous), 2- Fe-Mn oxide shalls, 3- Fe-Mn oxides and relicts of amorphous silica (matrix). h) Colloform texture: 1- Fe-Mn oxides (nucleous), 2: microcrystalline quartz and amorphous silica, 3-Fe-Mn oxides and relict of amorphous silica matrix).

The thickness in the center of lenticular Fe,Mn ores in the Baft region varies from 3 to 12 m and decreases gradually towards the ends. Length varies from 20 to 80 m. Thickness of the vein manganese ore deposits is less than the lenticular ores and varies from 2 to 10 m, and the length is more than 25 m.

Most of the ore deposits have lenticular or layered morphology. They are found on the basaltic units. In some cases they are interbeded with basaltic layers. The veins are less common.

According to (Rona *et al*., 1983) if the hydrothermal solutions undergo some mixing with colder sea water during the ascending shallow stages of their circulation. It is possible for Fe-Mn oxides and hydroxides to precipitate (e.g., Mn ores lining veins within basalts). Therefore northern Behkan Mn ore deposit with crosscutting vein structure (Fig. 4c) can be formed by the above processes in a predischarge stage during the activity of the subseafloor hydrothermal system.

A submarine gossan of 0.5 ppm Au is found between pillowlavas, and also over 400,000 Tons of slags related to an ancient Cu+Zn massive sulfide deposit is found in Zaghdar area (Fig.3).

Massive sulfide deposits together with a distal Fe-Mn oxide, hydroxide are reported by Rona *et al*., 1983. Therefore Zaghdar Mn ore deposit with layerd structure (Table1) can be formed, during the activity of black smokers in a distal zone.

Samples and Analytical Method:

A total of 60 samples were collected from Mn and Fe-Mn ores and hosts rocks. Petrographic and mineralogical studies of the Mn – phases were carried out on polished and polished thin sections under a reflected light microscope. Qualitative analysis of phases were carried out on an X ray powder diffractometcr. Microprobe analyses were performed in the Iran Mineral Processing Research Center (IMPRC). X-ray analysis was conducted in Kerman University. Whole rock chemical analysis of major oxides, trace elements and REE from the Baft ophiolite manganese and ferromanganese ore was conducted using ICP-AES and ICP-MS at the Alschemex Company, Canada (Table 2).

Ore Geochemistry:

Based on the analysis of the ore samples, two manganese ore types are distinguished in Baft ophiolithic melange: (a) black Mn ore type with Mn/Fe > 1, and relatively high ΣREE and (b) brown Fe,Mn ore type with Mn/Fe < 1, and relatively low ΣREE.

The ranges and average analytical results of both ore types are given in Table 2. In terms of variations in their majors, traces and rare earth elements (REE), both ore types are relatively inhomogeneous. MnO ranges from 11.65-45.4 wt% (average 26.56 wt %) in black Mn ore type, and 0.12-16.6 wt% (average 7.14 wt%) in brown Fe-Mn ore type. Mn/Fe ratios of the black Mn ores (average 7.86) and brown Fe-Mn ores (average 0.42) are quite different. The avarage Mn/Fe ratios of both manganese ore types in Baft ophiolite are comparable with thos of sedex deposits (0.1< Mn/Fe < 10), as defind by (Nicholson *et al*., 1997). Major and trace element discrimination diagrams have been proposed by many workers to distinguish manganese ores of various origins (Bonatti *et al*., 1972; Toth, 1980; Crerar *et al*., 1982; Adachi *et al*., 1986; Peters, 1988; Choi and Hariya, 1992; Shah and Moon, 2007). Plot of data from Mn and Fe-Mn ores in Baft ophiolites on Fe-(Co+Ni+Cu)-Mn discrimination diagram of (Bonatti *et al*., 1972), Ni-Zn-Co discrimination diagram of (Choi and Hariya, 1992), Si vs Al discrimination diagram of (Peters, 1988) and Co/Zn vs Co+Ni+Cu of discrimination diagram of (Toth, 1980) indicates a hydrothermal origin for the Baft manganese ores (Fig. 6). Toth, 1980 used Co/Zn ratios to distinguish hydrothermal Mn deposits (0.15) from those of the hydrogenous deposits (2.5). The Co/Zn ratios in Baft Mn-Fe brown ore types vary between 0.0016-0.38 (average 0.14) suggesting a hydrothermal origin, while those of the black Mn ore types vary between 0.04-1.92 (average 0.30) which also indicates a mixed hydrothermal-hydrogenous source for the Mn-Fe ores.

In Figure 7 comparison is made between the REE patterns of the black and brown manganese ore types from Baft ophiolites, and those of Mn-nodules and hydrothermal manganese ores.

It is now understood that the hydrogenous ferromanganese deposits have undergone a multifold enrichment of rare earth elements, compared with their hydrothermal counterparts, with a distinct positive Ce anomaly in the former and a distinct negative Ce anomaly in the later (Goldberg *et al*., 1963; Bostrom, 1974; Bonatti, 1975). The pattern of the maximum and average samples from black Mn ore types is similar to those of typical of submarine hydrothermal deposits, with a negative Ce anomaly (Fig.7) and the pattern of brown Mn-Fe ore type with relatively low ΣREE and sm negative anomaly is also similar to those of hydrothermal deposits.

Hydrogenous deposits show relatively high REE while the REE of hydrothermal deposits are significantly lower (Hein *et al*., 1990; Usui and Someya, 1997). In this research the average of ΣREE black and brown ore types from Baft ophilolites (62.5 ppm) and (19.3 ppm) respectively, are very noticeable (Table 2 & 3), and both ore types are characteristics of exhalative hydrothermal source material. According to Nath *et al*., 1997

Table 2: Ranges and averages of chemical compositions of various type of manganese and ferromanganese ore in Baft ophiolitic mélange.

	Black ore										Black ore										
	G5	GN.1	BL3.	BM.1	KU4	S9	BU.6	K.4	GL.1	Average	BM.8	BL.6	G2	G1	G.3	BH.1	ZS.1	BH.5	BL.3	S.8	S2	Average
Major elements (Wt%)																						
SiO2	27.5	10.0	43	30.4	53.2	19.4	65.3	53.9	44.9	38.6	19.8	53.2	67.4	55.4	75.3	53.8	26.2	6.31	66.5	59.4	37.9	49.2
Al2O3	1.49	1.68	0.23	0.70	1.45	5.59	0.08	0.19	11.2	2.51	1.17	1.72	0.17	0.15	0.05	0.01	1.72	0.36	0.04	13.7	3.78	1.92
Fe2O3	12.8	1.04	8.49	13.7	17.7	2.56	2.44	16.1	10.4	9.84	32.5	16.5	13.6	17.4	13.3	26.5	61.8	20.5	29.3	7.00	44.9	24.7
MnO	45.4	35.8	33.9	30.0	22.2	22.3	19.9	17.8	11.6	26.5	16.6	13.1	8.63	7.87	7.50	6.87	5.75	5.17	1.62	1.59	0.12	7.14
BaO	1.30	1.20	0.86	0.01	1.83	2.19	0.67	1.71	1.41	1.24	1.19	0.50	0.14	1.12	0.03	0.19	0.20	0.20	0.01	0.01	8.85	1.25
Mn/Fe	3.88	37.7	4.39	2.40	1.38	9.54	9.03	1.21	1.23	7.86	0.56	0.87	0.69	0.49	0.62	0.26	0.1	0.27	0.06	0.06	0.00	0.42
Terace elements (ppm)																						
Co	62.5	48.4	18.3	51.5	43	219	2.9	39.8	43.3	58.7	18.9	15.7	23.4	22.3	8.9	12.5	16.6	10.4	10.8	10.8	2.1	14.8
Cu	19	78	76	69	127	466	23	105	571	157	12	47	83	37	14	97	5050	54	5	5	15	474
Ni	131	316	104	174	115	83	26	143	334	158	5	20	223	78	82	91	5	5	15	15	20	53.8
Zn	159	440	170	283	185	114	74	172	125	191	87	68	162	148	192	220	10000	203	28	28	21	953.
Th	1.39	0.74	0.21	0.96	0.14	4.49	0.05	0.09	0.52	1.52	0.13	0.05	0.45	0.08	0.05	0.16	0.30	0.40	0.05	0.05	1.62	0.37
U	0.97	0.59	0.45	0.88	1.65	3.05	0.12	1.16	1.85	1.19	1.2	1.48	0.26	0.80	0.51	1.08	2.12	0.31	0.15	0.15	2.24	0.94
Rare earth elements (ppm)																						
La	19.3	8.80	7.00	17.6	21.2	28.7	5.00	13.9	35.4	17.4	2.00	0.5	3.4	4	0.7	3.1	2	3.3	0.50	4.8	28.5	4.64
Ce	20.5	9.60	2.7	16	1.5	26.4	0.5	0.7	41.2	13.2	2.3	0.6	5.1	1.5	0.5	1.6	2.2	5.4	0.9	9.1	50	6.64
Nd	11	5.6	6.4	9.4	10.3	18.1	1.3	7.7	35.1	11.6	1.3	0.2	2.1	1.5	0.4	2	1.9	2.9	0.5	6.7	22.6	3.52
Sm	2.07	1.14	1.24	1.75	2.21	3.49	0.2	1.31	7.99	2.35	0.26	0.04	0.43	0.3	0.3	0.41	0.13	0.42	0.11	2.01	4.61	0.73
Eu	0.78	0.48	0.4	0.51	0.72	1.2	0.12	0.64	3.08	0.87	0.25	0.05	0.16	0.2	0.04	0.18	0.18	0.17	0.06	0.74	2.54	0.38
Gd	2.61	1.55	1.42	2.43	1.9	4.7	0.33	1.7	9.9	2.9	0.39	0.14	0.52	0.57	013	0.7	0.55	0.63	0.12	2.67	4.15	0.89
Dy	2.39	1.47	1.28	2.41	1.65	5.5	0.33	1.46	9.92	3.36	0.25	.014	0.58	0.52	0.09	0.68	0.62	0.54	0.08	3.54	3.61	0.89
Er	1.64	1.10	0.74	1.86	1.21	5.13	0.21	0.86	6.09	2.08	0.24	0.13	0.41	0.51	0.08	0.6	0.42	0.4	0.09	2.38	1.9	0.61
Yb	1.29	0.94	0.55	1.53	0.72	5.75	0.2	0.65	4.69	1.80	0.16	0.15	0.37	0.41	0.07	0.51	0.40	0.32	0.1	2.12	1.52	0.52
Lu	0.19	0.13	0.07	0.26	0.12	1.03	0.03	0.09	0.83	0.29	0.04	0.03	0.09	0.09	0.03	0.09	0.05	0.07	0.05	0.31	0.22	0.09
La/Ce	0.94	0.91	2.7	1.1	14.1	1.08	10	19.8	0.85	5.7	0.86	0.83	0.66	2.66	1.4	1.93	0.9	0.61	0.55	0.53	0.57	1.55

Table 3: REE abundance in Ferromanganese ore deposits and other sedimentary materials (ppm) (Modified after Fleet and Robertson, 1980).

	La	Ce	Pr	Nd	Sm	Eu	Gd	Tb	Dy	Ho	Er	Tm	Yb	Lu	∑REE
Hydrogenous deposits (Ehrlich, 1968)															
Average	150	1460	57	200	55	12		7.5	44	7.3		2.8	15	2.7	2013
Max (Indian Oceanic)	237	2800		306	77.5	22	22		10.5			3.6	23	3.9	3505
Min (Pacific Ocean)	5.4	60		11	1.88	0.46		0.32				0.16	0.82	0.18	80
Hydrothermal deposits Average(Elderfield, 1981)	100	40		91	20	4.6							16		271.6
Max (Piper & Greaf, 1974)	182	93.7		159	28.3	6.16		5.42					18.3	3.21	495.4
Min (Bonnot & Courtois, 1981)	4	1.87		2.4	0.4	0.1		0.09					1.1	0.25	10.22
North American shale composite (Haskin et al, 1968)	32	73	7.9	33	5.7	1.24	5.2	0.85	5.8	1	3.4	0.5	3.1	0.48	173
Planktonic Foraminifer (Elderfield et al, 1981)	1.3	0.36		1	0.2	0.06	0.3		0.3		0.27		0.28		4.07
Seawater(X10-^{7}) Average of 11 sample of North Atlantic deep water (Hogdahl et al, 1968)	34	1	6.4	28	4.5	1.3	7.0	1.4	9.1	2.2	8.7	1.7	8.2	1.5	1.26
Basal umber, Skouriotissa, Cyprus	95	24.3		95.2	20.7	5.1		2.8				1.3	7.9	1	253.3
& Mn mineralization , Upennine ophiolite, Italy (Robertson and fleet, 1976)	1.7	5		2.7	0.7	0.2							0.2	1.8	12.3
Baft samples															
Average	11.1	9.9	4.2	7.6	1.6	0.62	1.9	0.88	0.7	1.1	1.35	0.42	1.15	0.16	42.68
Max	35.4	41.2	8.4	35.1	7.99	3.08	9.9	1.7	9.92	2.1	6.09	0.82	4.69	0.83	167
Min	0.5	0.6	0.1	0.2	0.04	0.05	0.1	0.06	0.14	0.1	0.13	0.02	0.14	0.03	2.09

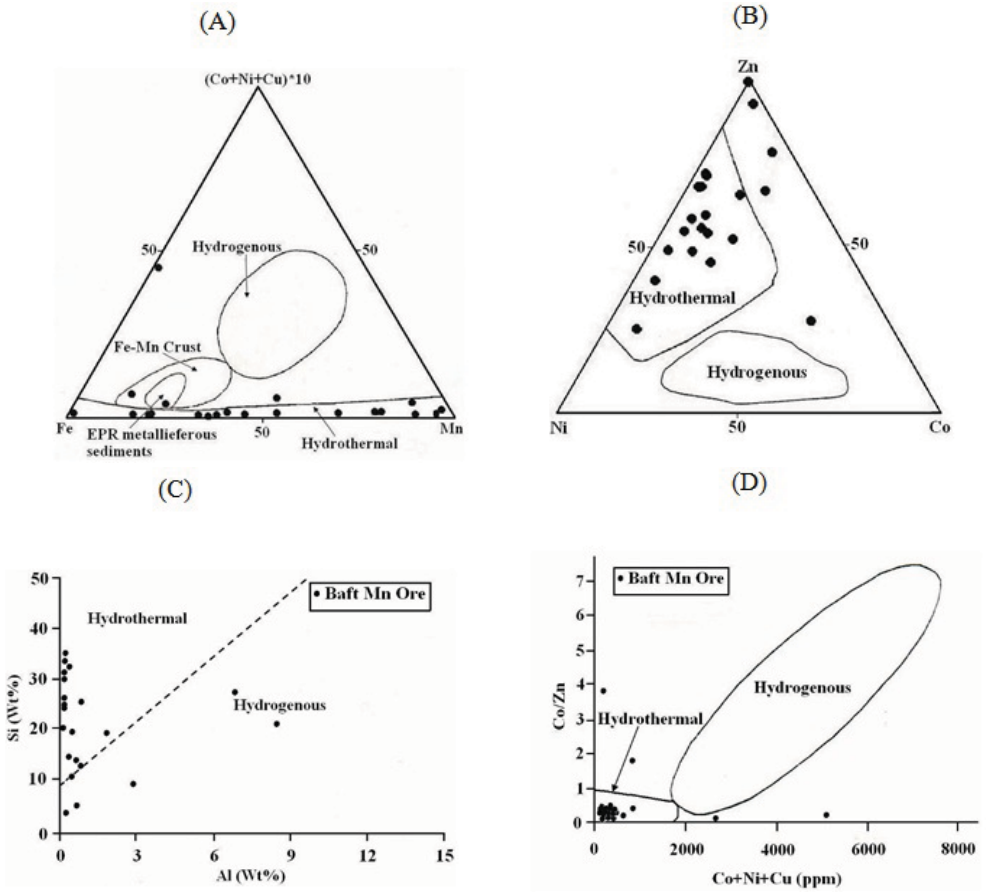

Fig. 6: Plot of Baft Mn and Fe-Mn ores on: (A) Mn-Fe-(Ni + Co + Cu)×10 discrimination diagram (Bonatti *et al*., 1972), (B) Zn-Ni-Co discrimination diagram (Choi and Hariya, 1992), (C) Si vs. Al discrimination diagram (Peters, 1988) and (D) Co/Zn vs. Co + Ni + Cu (Toth, 1980).

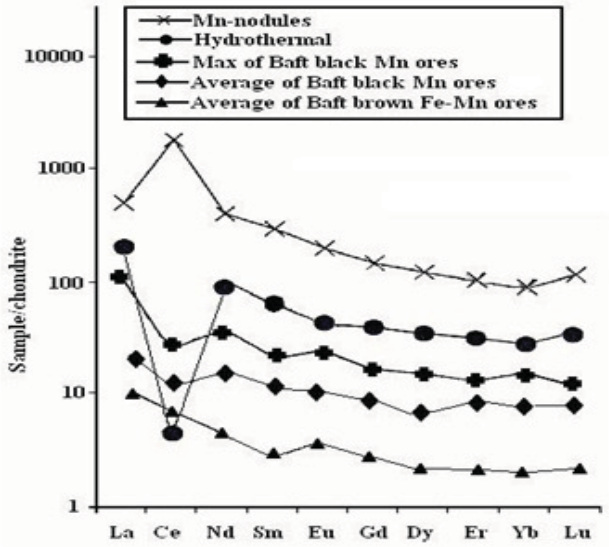

Fig. 7: Chondrite-normalized rare earth element data for the Baft manganese and ferromanganese ores compared with the average nodules and hydrothermal Mn ores (Ruhlin and Owen, 1986).

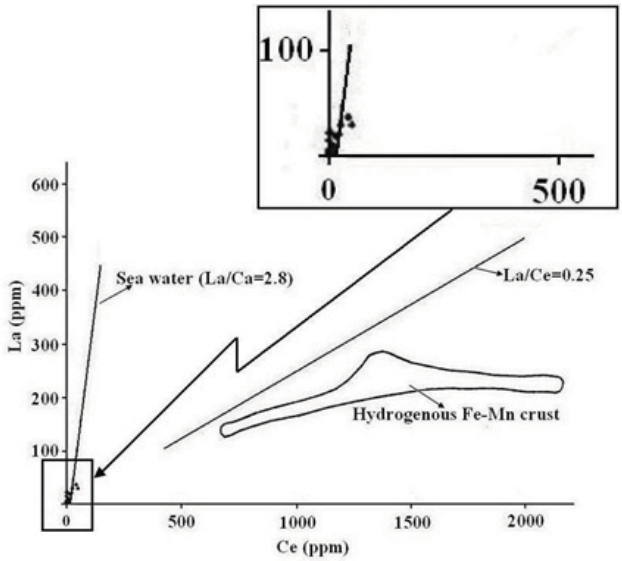

Fig. 8: Plot of Baft Mn and ferromanganese ores on the La vs. Ce discrimination diagram (Toth, 1980; Nath *et al.,* 1997).

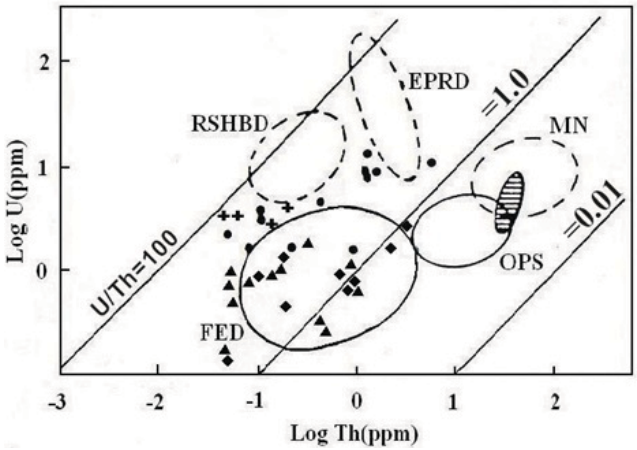

Fig. 9: Plot of Baft manganese and ferromanganese ores on the U vs. Th discrimination diagram of Rona, 1983.

MN= manganese nodules.
OPS= ordinary pelagic sediments.
Small shaded field= bauxites.
RSHBD= Red sea hot brine deposits.
EPRD= East Pacific Rise deposits.
FED= Fossil exhalative deposits.
Circles = hydrothermal crusts near spreading centers.
Crosses = represent ophiolitic Fe-Mn deposits probably of an
Exhalative-sedimentary origin.
◆=Baft black manganes ores.
▲=Baft brown Fe-Mn ores.

hydrothermal crusts have La/Ce ratios similar to seawater (~2.8), while hydrogenous Mn-Fe crusts have a much lower La/Ce ratio (~0.25). The La/Ce ratios for the Baft Mn-Fe ores vary between 0.53- 19.8 (average 3.32) (Table 2; Fig.8). This ratio is also in favour of a major input from a hydrothermal source for the Baft manganese and Ferromonganes ores.

In Fig.9 Mn ore samples from Baft region plot in the fossil exhalite field of the Th vs U discrimination

diagram of (Rona *et al*., 1983).

The U/Th ratios in Baft Mn and Fe-Mn ores vary between 0.68-29.6 (average 1.61). According to Bonatti 1975, U/Th>1 in submarine manganese ore deposits shows a high velocity of Mn precipitation and the lack and minor detrital input and therefore, this U/Th ratios of Baft Mn ores favor a major input from a hydrothermal source.

Factors Controlling the Formation of Baft Mn and Fe-Mn Ores:

Major and trace element, REE data, and morphology of the bodies (lenticular and vein type) of the Baft manganese and ferromanganese ores suggest that they are originated in an environment similar to those of the present day hydrothermal seafloor spreading centers. These ores could have been formed along and near to the mid-ocean ridges, from the hydrothermal solutions resulting from the interaction of the heated sea water and basic ignouse rocks beneath the sea floor. Mn and Fe were leached from the basaltic rocks which were finally discharged on to the sea floor (Bonatti, 1975; Crerar *et al.,* 1982). The Mn-Fe ores of Benehavuieh and Zaghdar areas, with a relatively high iron content (26.5 – 61.8 wt % Fe_20_3), and Mn ores of Northern Gelsorkhoo and Behkan areas,with a low iron content (1.04-2.44 wt% Fe203), suggest variable precipitation of Fe and Mn phases, due to Fe-Mn fractionation. According to Panagos and Varnavas, 1984, Mn compounds are more stable than iron compounds and, therefore Fe precipitates first, close to the source, whereas Mn remains in solution longer, Eh and/or pH also play a major role in the fractionation of Fe and Mn phases precipitate during the migration of solutions away from the vent, due to a gradual increase of Eh and/ or pH (Krauskopf, 1975; Hem, 1972; Roy, 1992). As the Mn ores are formed in close proximity to the souece of hydrothermal solution, while the Fe ores are formed more distally from the source, therefore, they attain different locations with respect to the exhalation center.The manganese ore deposits were later obducted on the land as a part of the Baft ophiolite complex. They can be compared with other ophiolite complexes such as the Apennine ophiolitic complex, Italy (Bonatti, 1975), the Semail Nappe, Oman (Fleet and Robertson, 1980), the Olympic Peninsula, USA (Crerar *et al.,* 1982; Chyiet *et al.,* 1984), and the Troodos complex of Cyprus (Robertson and Boyle, 1983) and the Vaziristan ophiolite of Pakistan (Shah and Moon, 2007).

AKCNOWLEDGEMENTS

The author is very gratful to the anonymous reviewers of AJBAS for their helpful and constructive comments. This paper is part of a project supported by Shahid Bahonar University.

REFERENCES

Adachi, M., K. Yamamoto, R. Sugisaki, 1986. Hydrothermal chert and associated siliceous rocks from the modern Pacific: their geologic significance as indication of ocean ridge activity. Sedimentary Geology, 47: 125-148.

Arvin, M., P.T. Robinson, 1994. The petrogenesis and tectonic setting of lavas from the Baft ophiolitic Melange, southwest of Kerman, Iran. Canadian journal of Earth Sciences, 31: 824-834.

Bonatti, E., 1975. Metallogenesis at oceanic spreading centers. Annual Review of Earth and Planetary Science, 3: 401-433.

Bonatti, E., T. Kraemer, H. Rydell, 1972. Classification and genesis of submarine iron-manganese deposits. In: Horn, D. (Ed.), Ferromanganese Deposits on the Ocean Floor: International Decade of Ocean Exploration. National Science Foundation, Washington, DC, pp: 149-166.

Bostrom, K., 1974. The origin and fate of ferromanganoan active ridge sediments. Stockholm Contributions to Geology, 27: 149-243.

Choi, J.H., Y. Hariya, 1992. Geochemistry and depositional environment of Mn oxide deposits in Tokoro belt, northeastern Hokkaido, Japan. Economic Geology, 87: 1265-1274.

Chyiet, M.S., D.A. Crerar, R.W. Carlson, R.F. Stallard, 1984. Hydrothermal Mn-deposits of the Franciscan assemblage, II. Isotope and trace element geochemistry, and implications for hydrothermal convection at spreading centres. Earth and Planetary Science Letters, 71: 31-45.

Crerar, D.A., J. Namson, M.S. Chyi, L. Williams, I.M. Feigenson, 1982. Manganiferous cherts of the Franciscan assemblage: general Geology, ancient and modern analogues, and implication for hydrothermal convection at ocean spreading centers. Economic Geology, 77: 519-540.

Davoudzadeh, M., 1972. Geology and petrography of the area north of Nain, central Iran, Geological survey of Iran, report No.39.

Fleet, A., A.H.F. Robertson, 1980. Ocean-ridge metalliferous and pelagic sediments of the Semail Nappe, Oman. Journal of the Geological Society, London, 137: 403-422.

Goldberg, E.D., M. Loide, R.A. Schmitt, R.H. Smith, 1963. Rare earth distributions in the marine environment. Journal of Geophysical Research, 68: 4209-4217.

Hassanipak, A., M. Ghazi, 2000. Petrology, geochemistry and tectonic setting of the Khoy ophiolite, northwest Iran: implications for Tethyan tectonics, J. Asian Earth Sci., 18: 109-121.

Hein, J.R., M.S. Schulz, J.K. Kang, 1990. Insular and submarine ferromanganese mineralization of the Tongap-Lau region. Marine Mining, 9: 305-354.

Hem, J.D., 1972. Chemical factors that influence the availability of iron and manganese in aqueous systems. Geological Society of America Bulletin, 83: 443-450.

Houshmandzadeh, A., M. Berberian, 1994. Geological quadrangle map of Hajiabad, Scale 1:250000: Iran Geol. Survey.

Krauskopf, K.B., 1957. Separation of manganese from iron in sedimentary processes. Geochimica et Cosmochimica Acta, 12: 61-84.

Mijakovic, N., S. Cvetic, 1972. Geological quadrangle map of Balvard, Scale 1:100000: Iran Geol. Survey.

Nath, B.B., W.L. Pluger, I. Roelandts, 1997. Geochemical constraints on the hydrothermal origin of ferromanganese incrustations from the Rodriguez triple junction, Indian Ocean. In: Nicholson, K., Hein, J.R., Bu¨hn, B., Dasgupta, S. (Eds.), Manganese Mineralization: Geochemistry and Mireralogy of Terrestrial and Marine Deposits. Geological Society, London, (Special Publication 119), pp: 199-21.

Nicholson, K., V.K. Nayak, J.K. Nanda, 1997. Manganese ores of the Ghoriajhor-Monmunda area, Sundergarh District, Orissa, Inida: geochemical evidence for a mixed Mn source. In: Nicholson, K., Hein, J.R., Bu¨hn, B., Dasgupta, S. (Eds.), Manganese Mineralization: Geochemistry and Minralogy of Terrestrial and Marine Deposits. Geological Society, London, (Special Publication 119), pp: 117-121.

Panagos, A.G., S.P. Varnavas, 1984. On the genesis of some manganese deposits from eastern Greece. In: Wauschkuhn, A., Kluch, C., Zimmerman, R.A. (Eds.), Syngenesis and Epigenesis in the Formation of Mineral Deposits. Springer, Berlin, pp: 553-561.

Peters, T., 1988. Geochemistry of manganese-bearing cherts associated with Alpine-ophiolites and the Hawasina formations in Oman. Marine Geology, 84: 229-238.

Robertson, A.H.F., J.F. Boyle, 1983. Tectonic setting and metalliferous sediments in Mesozoic Tethys Ocean. In: Rona, P.A., Bostrom, K., Laubier, L., Smith Jr., K.L. (Eds.), Hydrothermal Processes of Sea-floor Spreading Centres. Plenum Press, NY, pp: 595-663.

Rona, P., K. Bostrom, L. laubier, K. Smith, 1983. Hydrothermal processes at Sea floor spreading centers. Published in cooperation with NATO Scientific Affairs Division, pp: 796.

Roy, S., 1992. Environments and processes of manganese deposition. Economic Geology, 87: 1218-1236.

Roy, S., 1997. Genetic diversity of manganese deposition in the terrestrial geological record. In: Nicholson, K., Hein, J.R., Bu¨hn, B., Dasgupta, S. (Eds.), Manganese Mineralization: Geochemistry and Mineralogy of Terrestrial and Marine Deposits. Geological Society, London, (Special Publication 119), pp: 5-27.

Ruhlin, D.E., R.M. Owen, 1986. The rare element geochemistry of hydrothermal sediments from the east Pacific rise: examination of a seawater scavenging mechanism. Geochimica et Costmochemica Acta, 50: 393-400.

Shahabpour, J., 2005. Tectonic evolution of the orogenic belt in the region located between Kerman and Nyriz. J. Asian. Earth. Sci., 24: 405-417.

Shahabpour, J., 2002. Economic Geology. Shahid Bahonar Univercity of kerman Publications, 137: 543.

Shah, M.T., C.J. Moon, 2007. Manganese and Ferromanganese ores from different tectonic settings in the NW Himalayas, Pakistan. Journal of Asian Earth Sciences, 29: 455-465.

Toth, J.R., 1980. Deposition of submarine crusts rich in manganese and iron.Geological Society of America Bulletin, 91: 44-54.

Usui, A., M. Someya, 1997. Distribution and composition of marine hydrogenetic and hydrothermal manganese deposits in the northwest Pacific. In: Nicholson, K., Hein, J.R., Bu¨hn, B., Dasgupta, S. (Eds.), Manganese Mineralization: Geochemistry and Mineralogy of Terrestrial and Marine Deposits. Geological Society, London (Special Publication 119), pp: 177-198.